

## 4

## CFD Simulation of Wind-Induced Interference Effects on Low-Rise Gable Roof Structure using ANSYS

Aman Kumar Chaurasia, Animesh Kumar Anand, Anuved Meena, Deepak Sharma, Ritu Raj\*

Department of Civil Engineering, Delhi Technological University, Delhi, India

\*Corresponding author email: rituraj@dtu.ac.in

### Abstract

This study examines the variance of wind impacts on low-rise gable-roofed buildings that do not have any open faces to the wind domain over distinct interference situations. In full blockage arrangements, this is achieved by adjusting the spacing between the buildings. Because there are no specifications in wind standards for building structures of this kind, computational simulations are carried out using the fluid flow simulator of ANSYS CFX software using the Standard  $k - \epsilon$  model. These kinds of research necessitate the use of either a real wind tunnel environment to measure the pressure or a virtual computational fluid dynamics (CFD) simulation of the wind environment. In this work, CFD simulations were performed for a total of four distinct spacing circumstances and four varied increasing wind incidence angles of  $0^\circ$ ,  $30^\circ$ ,  $60^\circ$ , and  $90^\circ$  to get the coefficient of pressure ( $C_p$ ). The results have been showed with the help of contours on the roofs of structures, pressure coefficient ( $C_p$ ) and velocity streamlines for different cases. Minimum value of  $C_p$  was found in 1.5b spacing configuration with wind incidence angle  $60^\circ$  and maximum value of  $C_p$  in 2b spacing configuration with wind incidence angle  $60^\circ$  (here b = width of structure).

### Keywords

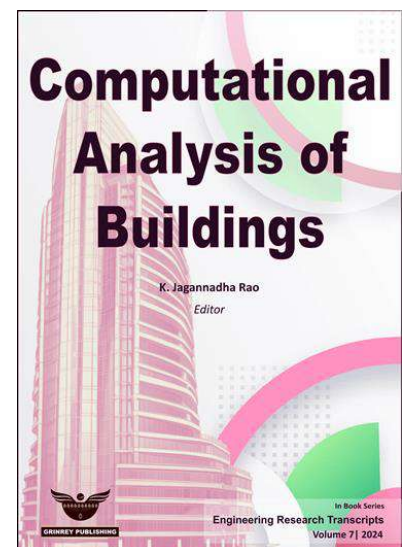
ANSYS CFD Simulation, Gable Roof, Wind Interference

Received: 25 Mar 2023 | Accepted: 03 Mar 2024 | Online: 08 Mar 2024

### Cite this article

Aman Kumar Chaurasia, Animesh Kumar Anand, Anuved Meena, Deepak Sharma and Ritu Raj (2024). CFD Simulation of Wind-Induced Interference Effects on Low-Rise Gable Roof Structure using ANSYS. *Engineering Research Transcripts*, 7, 63–74.

DOI: [https://doi.org/10.55084/grinrey/ERT/978-81-964105-4-4\\_4](https://doi.org/10.55084/grinrey/ERT/978-81-964105-4-4_4)



## 1. Introduction

The need for structures such as factories, warehouses, godowns, refrigerated storage, bunkers, and so forth has increased as a result of the global economic development and extensive industrialization. Rapid globalization is made possible in large part by the air transportation network. Hangars are important buildings at airports that are used for maintaining, repairing, and storing aircraft. These buildings have truss roofs and enormous plan proportions. Such roofs are greatly impacted by wind, and this must be carefully considered. Strong winds have caused several roof structures to disintegrate in recent years. Hurricanes and other strong wind events frequently cause low-rise structures in coastal areas to sustain considerable damage. The first areas of these damages are high pressure areas or weak building components, and they spread to other building components. In addition, depending on the arrangement, design, positioning with relation to the streamlines and terrain in the upstream, neighboring structures can lessen or raising the induced flow force applied on a building. As a result, designers and planners must correctly examine this effect, known as interference, and it is typically observed in metropolitan areas where clusters of buildings are built at a site. When several structures are included, the analysis becomes more complex due to the enormous quantity of observations accessible. As a result, the interference factor, that is a useful tool for analyzing how wind behaviour and pressure on the other structure change, is known as the ratio between the pressure coefficient at a specific structural adaptation to the pressure coefficient on a similar structure in a remote setting of similar shape with similar boundary conditions.

When creating other structures that are subject to wind loads. Wind load standards are used by designers to calculate coefficients of force and pressure for the structure [1]. These standards, on the other hand, include information for element configurations with a few restricted wind incidence angles. Information on wind loads for structures with varied configurations is not provided by these regulations. As a result, it is highly common to investigate wind tunnels using models of this form. Many researchers have already looked into effects of wind on small buildings. For instance, Jagbir and Roy [2] used numerical modelling to look into the a small structure's wind loads roof and discovered that they are restricted for structures with pyramidal shapes. In an experiment conducted by Boumrar and Becheur (2020) [3], it was discovered that the design and slope of the roof had a positive impact on the aerodynamic properties of tall structures by reducing the drag force on the windward face. In their assessment of wind pressures on awnings attached to small buildings, Sakib (2021) [4] discovered that awnings are most impacted by suction pressure, which is primarily felt on the top portion of the top of buildings. In 2019, Ong [5] looked into the average and maximum pressure caused by wind around a low-rise building. In comparative research on minimising uplift force on low-rise structures, Aly and Bresowar (2016) [6] recommended that aerodynamic mitigation should also reduce the structure's drag and lift forces in addition to the pressure coefficient. By altering the ratios of height to depth and breadth to depth, Huang (2018) [7] assessed the air pressure in a several testing on various types of roofing in the wind tunnel. The existing international criteria for low-rise structures need to be revised in light of the many pieces of accessible data. Full scale assessment on low rise structures under actual wind conditions was done by Kopp (2012)[8] . Isyumov (2014) [9] used a low-rise building model to conduct an experimental analysis utilising wind tunnel testing at various wind incidence angles. The prevailing wind pattern all around low-rise building is not addressed in the international standards that are available for its design. Additionally, the pattern of pressure distribution must be taken into account. Wind effect study on low-rise (small ) structures of dome shape have been done by Astha and Rahul [10] and they found out that single dome has maximum pressure at the peak. Ahmad and Kumar (2001) [11] conducted wind tunnel studies on hip roofs and found that interference effects provide appreciable improvements and shielding benefits at various configurations. Nagar (2020 and 2021) conducted experimental tests on proximity effects caused by wind among two high rise buildings in many blocking configurations that were

plus-shaped, square, and H-shaped [12-13]. Wind effects with one side open on low rise structures were done by Sinha et al (2022) [14] for full blockage interference conditions. Shruti et al (2019) studied the interference effect on chimneys under different wind incidence angles. [15]

IS 875 (Part 3): 2015 Indian Standards criteria for estimating wind loads on structures were thoroughly studied, and the regulations were referenced to at various stages.

This study utilizes a low-rise rectangular structure with having gable roof and no open sides to assess how changing the distance between structures affects the force of the wind against the roof.

The impact on the building close to another structure may cause its wind load to either increase or decrease. The wind load enhancement effect and the shielding effect are two distinct ideas. The influence that will predominate will depend on where and how the structures are positioned in relation to the wind's direction. The results of wind-induced interference are quantified in this CFD analysis for a range of spacing configurations and wind flow directions.

## 2. CFD Simulation Methodology

There are several types of commercial software available for CFD simulations. One of the most popular software packages, Ansys, includes a variety of tools for engineering simulation. The easiest solution for CFD studies of wind flow across bluff bodies is Ansys CFX. As a result, the simulations for this inquiry were carried out using the k- $\epsilon$  turbulence model at higher turbulence strength in the Ansys 2022 R2 CFX fluid flow package. This is the turbulence model that is most frequently used in Computational Fluid Dynamics studies of wind flow across bluff bodies. Here, the terms k and  $\epsilon$  represent for the TKE (turbulent kinetic energy) and the rate of eddies in the wind that a bluff body's presence causes, respectively.

Five fundamental steps are used in CFD simulations, and they are as follows:

- Creating the model's geometry
- Setting up a flow domain,
- Discretize or mesh a domain.
- Establishing boundary conditions and flow physics,
- Coming up with solutions

A 3D modeling programme, in this case AutoCAD, was used to model the structure under consideration. Then, in order to simulate a wind tunnel, a fluid flow domain must be created around the structure. This was accomplished using ANSYS' Design Modeller tool. The discretization of the flow domain, generally defined as the meshing of the flow domain, occurs in CFD simulations. These components can have a variety of forms, including pyramidal, tetrahedral, hexahedral, and hexagonal. The flow's continuance and momentum are equal along every node of the discretized domain according to the Reynolds averaged Navier-Stokes equation. Tetrahedral meshing was used in the current study. To create a high-quality mesh, the element sizes throughout the meshing process must be modified.

The next steps consist of setting the boundary conditions and defining the wind profiles that will apply the force on the building. Free slip walls were allocated for the domain's top and bottom walls. ( $\tau_{\text{wall}}=0$  &  $V_{\text{wall}}\neq 0$ ), where  $V_{\text{wall}}$  stands for velocity along a wall's surface and  $\tau_{\text{wall}}$  for the wall's shear stress. However, there is no velocity component that is perpendicular to the surface. At the borders of the virtual wind tunnel, this is done to emulate free stream flow circumstances found in nature. Because no-slip walls ( $V_{\text{wall}}=0$ ) were selected for the building faces and the ground. there is no fluid velocity component around the wall's perimeter. The nonslip wall criterion makes sure that air flow encounters viscous friction from the ground

and the structure's faces. The definition of corresponding pressure at the output was 0 Pa. In the current investigation, the domain's entrance is equipped with a constant, homogeneous wind flow moving at a speed of 10 m/s. After the flow setup is complete, the momentum and continuity equations are repeatedly solved at every node of the mesh by the ANSYS solution operator. As the number of iterations rises, less momentum and mass are left behind each way along, and the solution eventually reaches the final state. ANSYS CFD post-tool allows users to obtain the results after the solution is finished. By using streamlines, it is possible to see the entire flow around the body and determine the pressures and forces that act on the body's surfaces through the result file. Both the wind speed and the size of the model will affect the pressure and force magnitudes. It takes a dimensionless quantity to adequately depict the pressures and forces in a general sense.

The pressure coefficient, which defines the relative pressure at whatever place in relation to the design pressure, is a dimensionless quantity. It is defined mathematically using Equation (Eq). (1)

$$C_p = \frac{P - P_0}{\frac{1}{2} \times \rho \times V^2} \quad (1)$$

where the design wind speed and air density, respectively, are  $V$ , and  $P$  represents any location where there is wind pressure. To describe the wind pressure impacting on the structure's faces in dimensionless terms, use Eq. (1) to produce the expression for  $C_p$  in Ansys' built-in function calculator. To visualize the fluctuation of  $C_p$  throughout the various faces, the values of pressure coefficient  $C_p$  could alternatively be plotted  $C_p$  contours throughout the entire face.

### 3. Design of Structure

The experimental model for the current experiment is a low-rise rectangular design with gable roof structural model, scaled at 1:50. With a maximum horizontal wall length of 400mm and minimum wall length of 200mm, the pitched roof has a 30° pitch. According to Figure 1, the wall height of the building is 150 mm.

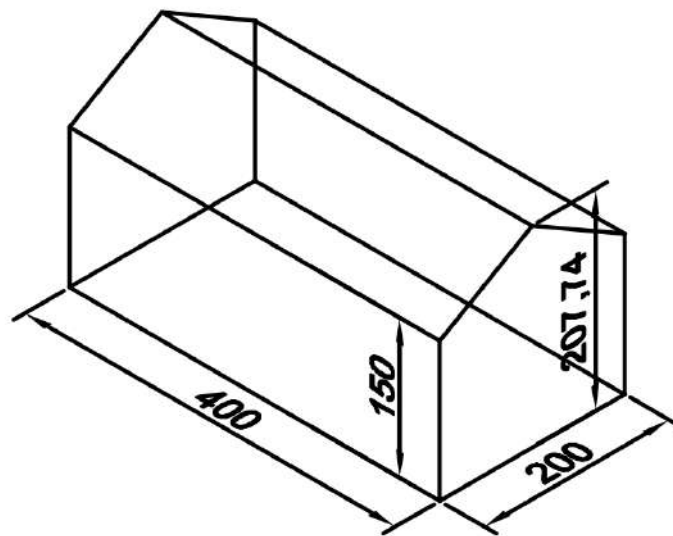


**Fig. 1.** Model of the structure (all dimensions in mm)

#### 4. Validation of Model with IS Code

A validation model that matched the flow setup's external measurements and meshing was exposed to the same typical wind velocity of 10 m/s at the inlet in order to verify the flow setup, as shown in Figure 2. The setup was assessed by contrasting the pressure coefficient ( $C_p$ ) values obtained by Ansys CFX to those derived from the IS codes for a covered gable roof structure (based on real wind tunnel tests).

For calculating the domain size, Franke et al. (2004) [16] followed their suggestions on CFD applications in wind engineering. The dimensions used for the wind flow domain are shown in Figure 2. The safe separations between the intake and outflow faces and the structure were  $5H$  and  $15H$ , respectively. The building's top and side clearances were taken to be  $6H$ .  $H$  denotes the structure's height and is equivalent to 207.74 mm.

As shown in Figure 3, the volume mesh size is taken as 0.1 m, whereas the mesh size for the building edges is 0.025 m, the mesh size for the face is 0.0125 m, and the mesh size for the ground is 0.05 m.

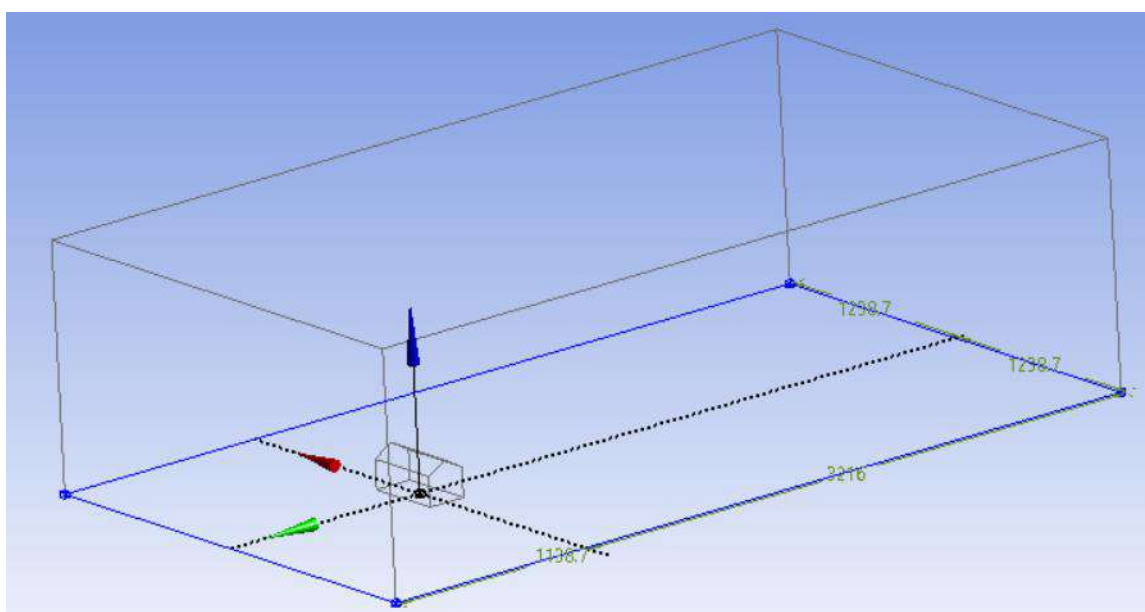


**Fig. 2.** Wind Flow Domain

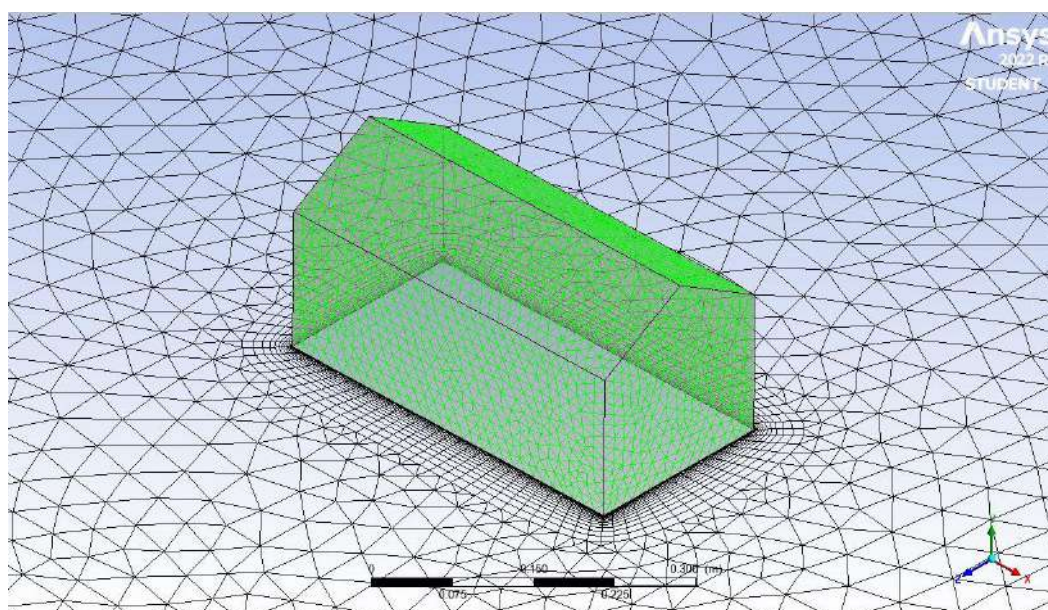


**Fig. 3.** Mesh Diagram

An average inaccuracy of percentage of 14.28% was found across the entire Top surfaces along the direction perpendicular to the model's longest side, this corresponds to the  $0^\circ$  wind incidence in IS 875 Part 3:2015, when comparing the average values of pressure coefficient acquired for the verification model with the values of pressure coefficient specified in clause 7.3.3.2 Table 6 of the IS 875 Part 3:2015. Since there are no openings in the structure, we can consider pressure coefficients to be external pressure coefficients.

**Table 1.** Verification of CFD Model Setup from IS 875 (Part 3): 2015

Wind Angle ( $\Theta^\circ$ )	$C_{pe}$ for surface from CFD Simulation		Average Value of $C_{pe}$ for Roof from CFD Simulation	Average Value of $C_{pe}$ for Roof as per IS 875 (Part 3) [Table 6 clause 7.3.3.2]	Average % Error
	Roof 1	Roof 2			
0	-0.41	-0.39	-0.4	-0.35	14.28

Suction develops in the areas along the margins as a result of the wind escaping from the bluff body's pointed edges. The high suction values close to the building's margins significantly raise the average suction  $C_{pe}$  because the CFD simulations capture the tiniest fluctuations in wind pressure similar to the size of the meshing elements. A discrepancy of 0.05 in the  $C_{pe}$  values is seen in the current investigation when comparing them to IS 875 part 3:2015.

Since the obtained results on the validation model fall under allowable bounds of the IS CODE, the same mesh generation and boundary setup were used for all simulations undertaken in this work.

As illustrated in Figure 4, the simulations are run for various distances between the experimental test model and the interfering model as well as various wind incident angles ranging from  $0^\circ$  to  $90^\circ$  at a  $30^\circ$  interval. In the current investigation, the interfering model is interpreted as being similar exterior measurements as the experimental test model. The distance between the two models is adjusted in terms of the building's width,  $b$  ( $= 200$  mm), while the experimental test model is kept directly at the back of the interfering model, or in a full blockage situation, at  $0^\circ$  wind incidence. As shown in Figure 5, there are four spacing configurations ( $S$ ) that were taken into account for this study:  $b/2$ ,  $b$ ,  $3b/2$ , and  $2b$ .

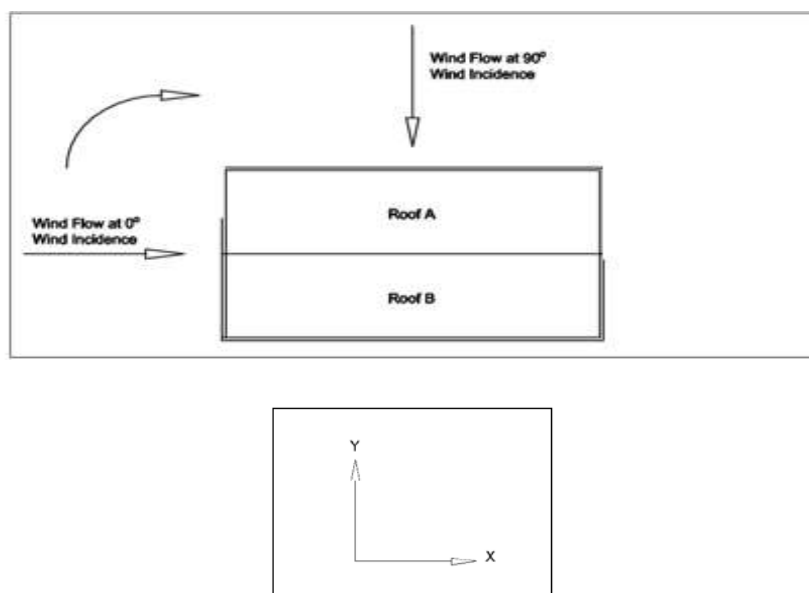
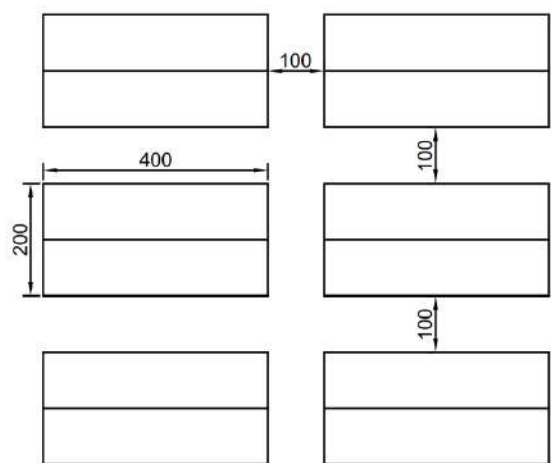
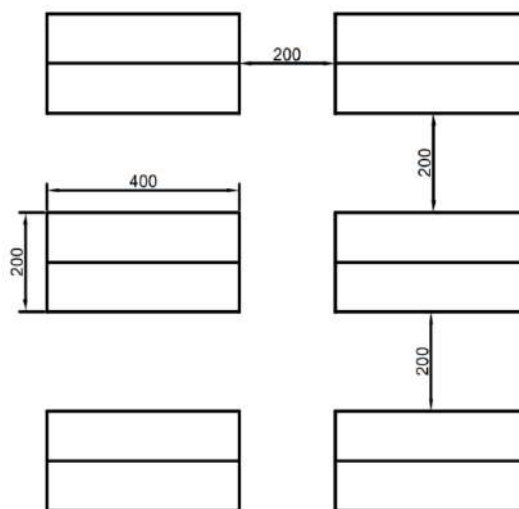


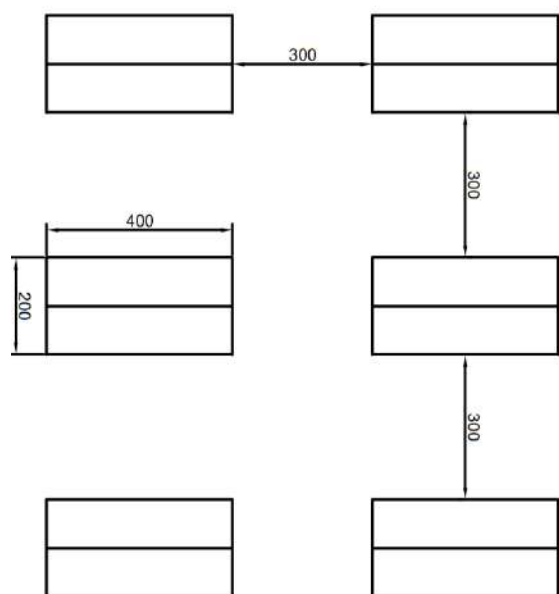
**Fig. 4.** Variation of Wind Incident Angles



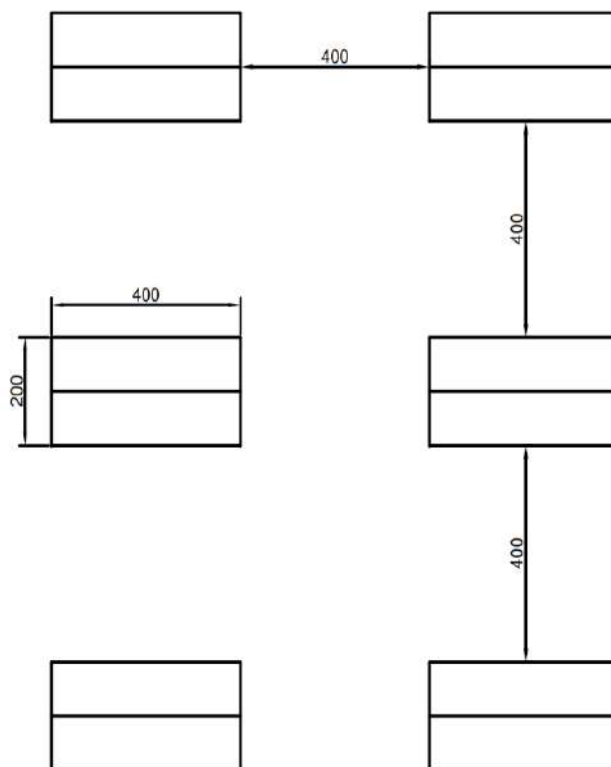
(a)  $b/2$  Spacing



(b)  $1b$  Spacing



(c)  $3b/2$  Spacing



(d)  $2b$  Spacing

**Fig. 5.** Spacing Configurations

## 5. Results and Discussion

### 5.1 Average Pressure Coefficient

Figure 6's graph illustrates the Coefficient of pressure mean variation in the entire gable roof with respect to wind incidence angles. Similar variations can be seen in the  $C_p$  mean graph for the exterior roof face in interference condition, which, for every spacing, is suction in nature.

Suction is evident in the isolated structure condition and it decreases as the wind incidence angle increases from 0 to 30 degrees, then it increases from 30 to 60 degree then again decreases from 60 to 90 degree. Particularly at 0°, the suction pressure is stronger at around -0.45 for the top, but in the other circumstances, the interference from the building causes eddy forms, which lowers the suction pressure. Similarly, the suction is also induced in the interference conditions on the top it increases as the wind incidence angle rises from 0° to 30° and it decreases from 30° to 90° for each spacing. The shielding effect of the interfering building results in a decrease in Coefficient of pressure mean values for the interference instances.

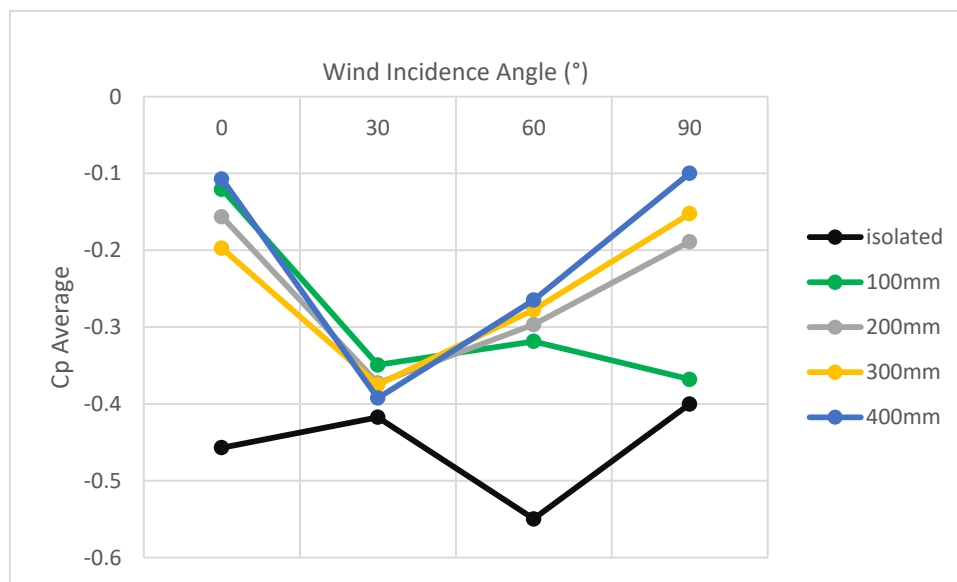


**Fig. 6.** Deviation of average pressure coefficient ( $C_{pe}$ ) with wind incidence angles

### 5.2 Interference Parameters

Wind-induced interference effects have been the subject of numerous studies. According to Khanduri et al. (1998) [17], the consequences of interference necessitate systematic research because the analysis study cannot be directly contrasted because of the various geometrical arrangements. As a result, utilizing the interference parameter - interference factor (IF), the current study examines how the wind action changes as buildings are separated from one another. Coefficients of pressure  $C_p$  for a building with the interfering building divided by the  $C_p$  for the same building under isolated conditions is known as interference factor (IF). These characteristics aid in numerically representing the effect of interfering building on the wind effect on the structure under consideration. Both positive and negative interference factor IF values are possible. Positive interference factor (IF) signals that the kind of the wind action, In an isolated situation, factors like pressure or suction are same. as well as in interference configuration, whereas negative IF signals a change in the wind action's nature. The building under consideration may have been shielded from wind activity by the interfering building if the interference factor's magnitude is less than one. If the magnitude of IF is greater than one, the existence of the interfering buildings is considered to be increasing the wind load.



We can observe on top 1 of the 0.5B spacing arrangement that the shielding impact on the interference building decreases as the wind incidence angle increases from  $0^\circ$  to  $90^\circ$  but for the 2B spacing configuration as we can see that sheltering effect has increased with change in wind incidence angle from  $0^\circ$  to  $90^\circ$  and positive wind pressure is observed at  $90^\circ$  on top 1 because there is a change in sign of IF value from positive to negative. A gradual increase in IF value can be seen for all four spacing configurations i.e., 0.5B, 1B, 1.5B, 2B at  $30^\circ$  wind incidence angle due to less sheltering been provided and then a gradual decrease in IF value for  $60^\circ$  wind incidence shows better sheltering.

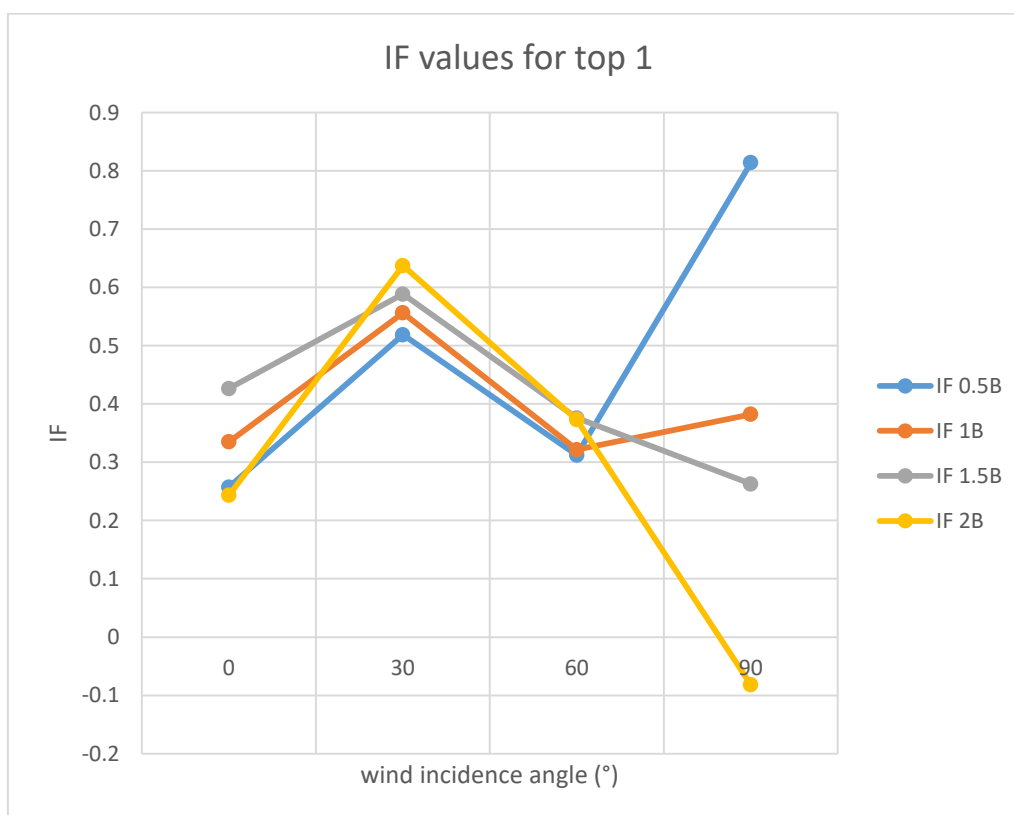
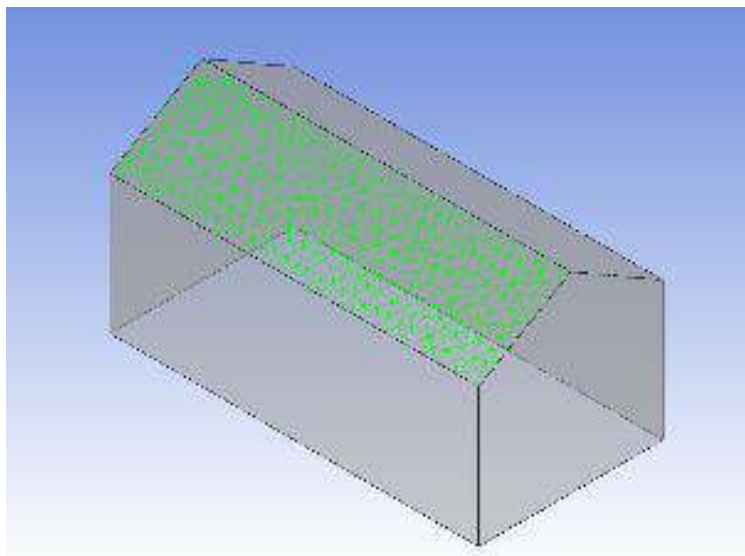


**Fig. 7.** Variation of interference factors on top 1 along wind incidence angle ( $^\circ$ ).

On top 2 for all spacing configuration, we can see that IF value is less 1 for  $0^\circ$  wind incidence angle and these values are in very close range of each other denoting very good sheltering effect at  $0^\circ$  wind incidence angle. But for wind incidence angle of  $30^\circ$  there is a sudden rise in IF values and all values of IF at  $30^\circ$  wind incidence angle becomes greater than 1 denoting there is a change in wind load action on top 2 of the interference building meaning more wind load is acting than the initial provided wind load on the top of building and this effect is gradually decreased with further increase in wind incidence angle till  $90^\circ$ . 1.5B spacing configuration has best sheltering effect compared to other spacing configurations for roof 2 of the interference building.

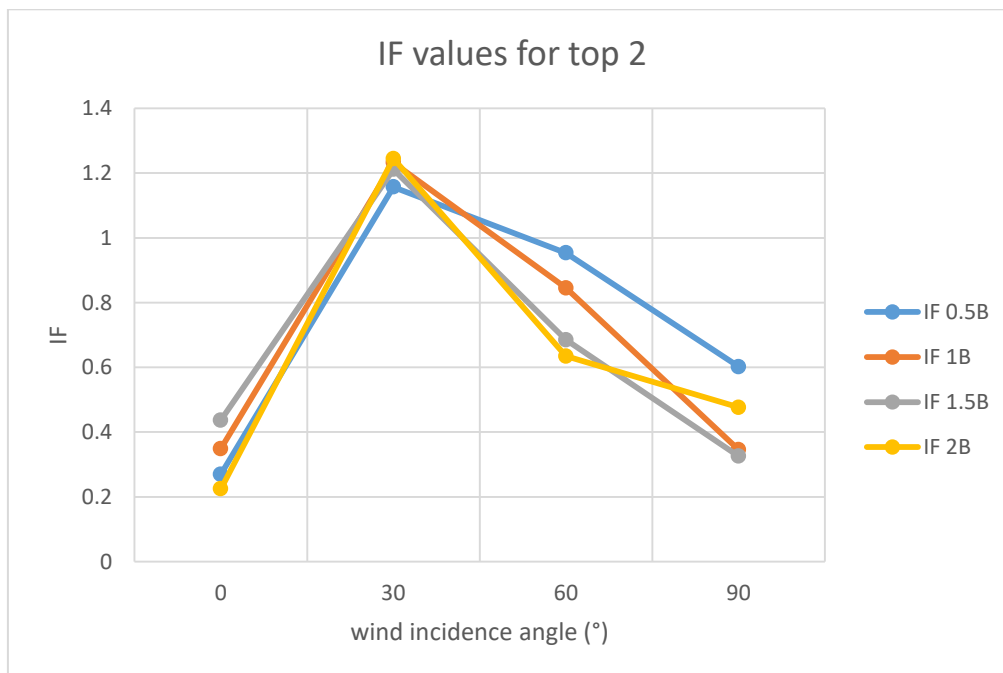
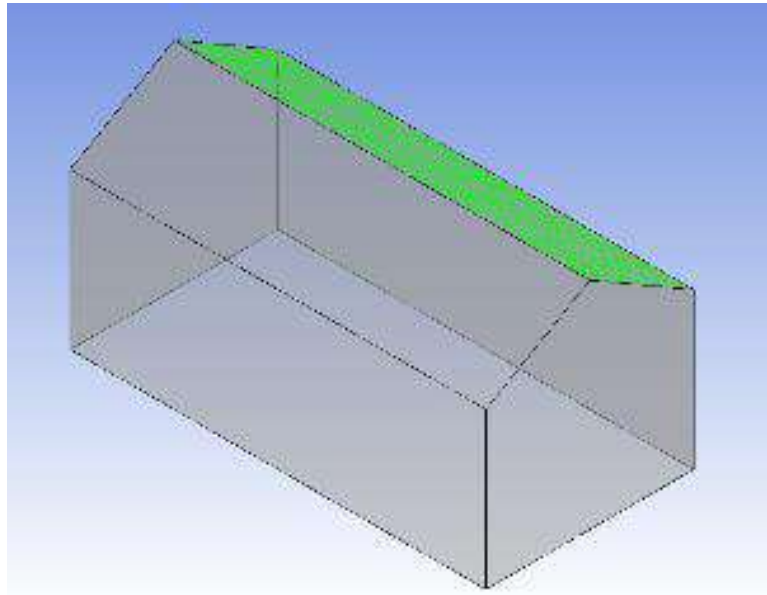


**Fig. 8.** Variation of interference factors on top 2 along wind incidence angle ( $^\circ$ ).

## 6. Conclusion

The basis for this research is the impact of changing the spacing configurations in an interfering wind flow scenario. In accordance with standards of IS 875: Part 3 (2015) requirements, the validation of the coefficients of pressure on the top of a gable roof design was carried out, and the outcomes of the CFD simulations were within acceptable bounds. In order to investigate the effects on the  $C_p$ , four distinct spacing configurations (depending on the structure width, i.e., at 0.5B, 1B, 1.5B, and 2B spacing) were assumed and also then compared this interfering condition with isolated wind flow circumstances via Interference parameter (IF). The important findings of this study are:

- For all interfering conditions, there is a similar fluctuation in the average value of the pressure coefficient for the structure's Top 1 and Top 2. All the roofs on average are in suction for low rise buildings meaning negative pressure is acting. For 30° wind incidence angle maximum suction of roof in different spacing configuration is observed.
- IF values increase from 0° to 30° wind incidence angle for all spacing configurations indicating a decrease in shielding effect on the experimental building, IF values then decrease for 30° to 90° wind incidence angle indicating a increase in shielding effect on the experimental building.

According to the findings of this study, the shielding effect is reduced at 30° wind incidence angle for all spacing configurations when compared to other wind incidence angles. It is therefore prudent to keep this discovery in mind while building similar style colonies.

This would assist in creating a thorough set of suggestions that could be incorporated into commonly used wind regulations like IS 875: Part 3(2015) and utilized in analyzing various interference scenarios.

To determine the appropriate spacing and orientations for these types of low-rise frameworks/buildings both in terms of serviceability and soundness as structures under varied airflow circumstances, ANSYS CFX simulations for interference parameters would be useful.

## References

- [1] IS 875, “IS 875 - Design Loads (Other than Earthquake) for Buildings and Structures-Code of Practice Part 3 Wind Loads (Third Revision),” 2015.
- [2] J. Singh, A. Kumar Roy, S. Jagbir, and R. Amrit Kumar, “Wind load on roof of low-rise building through CFD simulation,” 2021.
- [3] I. Boumrar and A. Becheur, “Roof slope effects on the aerodynamic characteristics of tall buildings,” *Engineering Review*, vol. 41, no. 2, Apr. 2020, <https://doi.org/10.30765/ER.1481>.
- [4] F. A. Sakib, T. Stathopoulos, and A. K. Bhowmick, “A review of wind loads on canopies attached to walls of low-rise buildings,” *Eng Struct*, vol. 230, p. 111656, Mar. 2021, <https://doi.org/10.1016/J.ENGSTRUCT.2020.111656>.
- [5] R. H. Ong, L. Patruno, D. Yeo, Y. He, and K. C. S. Kwok, “Numerical simulation of wind-induced mean and peak pressures around a low-rise structure,” *Eng Struct*, vol. 214, p. 110583, Jul. 2020, <https://doi.org/10.1016/J.ENGSTRUCT.2020.110583>.
- [6] A. M. Aly and J. Bresowar, “Aerodynamic mitigation of wind-induced uplift forces on low-rise buildings: A comparative study,” *Journal of Building Engineering*, vol. 5, pp. 267–276, Mar. 2016, <https://doi.org/10.1016/J.JOBE.2016.01.007>.
- [7] P. Huang, L. Tao, M. Gu, and Y. Quan, “Experimental study of wind loads on gable roofs of low-rise buildings with overhangs,” *Frontiers of Structural and Civil Engineering 2018 12:3*, vol. 12, no. 3, pp. 300–317, Jan. 2018, <https://doi.org/10.1007/S11709-018-0449-7>.

- [8] G. A. Kopp, M. J. Morrison, and D. J. Henderson, "Full-scale testing of low-rise, residential buildings with realistic wind loads," *Journal of Wind Engineering and Industrial Aerodynamics*, vol. 104–106, pp. 25–39, May 2012, <https://doi.org/10.1016/J.JWEIA.2012.01.004>.
- [9] N. Isyumov, E. Ho, and P. Case, "Influence of wind directionality on wind loads and responses," *Journal of Wind Engineering and Industrial Aerodynamics*, vol. 133, pp. 169–180, Oct. 2014, <https://doi.org/10.1016/J.JWEIA.2014.06.006>.
- [10] A. Verma, R. K. Meena, R. Raj, and A. K. Ahuja, "Experimental investigation of wind induced pressure on various type of low-rise structure," *Asian Journal of Civil Engineering*, vol. 23, no. 8, pp. 1251–1265, Dec. 2022, <https://doi.org/10.1007/s42107-022-00480-6>.
- [11] S. Ahmad and K. Kumar, "Interference effects on wind loads on low-rise hip roof buildings," *Eng Struct*, vol. 23, no. 12, pp. 1577–1589, Dec. 2001, [https://doi.org/10.1016/S0141-0296\(01\)00057-8](https://doi.org/10.1016/S0141-0296(01)00057-8).
- [12] S. K. Nagar, R. Raj, and N. Dev, "Experimental study of wind-induced pressures on tall buildings of different shapes," *Wind and Structures*, vol. 31, no. 5, pp. 431–443, Nov. 2020, <https://doi.org/10.12989/WAS.2020.31.5.431>.
- [13] S. K. Nagar, R. Raj, and N. Dev, "Proximity effects between two plus-plan shaped high-rise buildings on mean and RMS pressure coefficients," *Scientia Iranica*, vol. 29, no. 3, pp. 990–1005, Jun. 2022, <https://doi.org/10.24200/SCI.2021.55928.4484>.
- [14] A. Sinha, A. K. Jha, and R. Raj, "Wind-Induced Interference Effects on Low-Rise Pitched Roof Structure Based on CFD Simulations," *Journal of The Institution of Engineers (India): Series A*, Dec. 2022, <https://doi.org/10.1007/s40030-022-00675-9>.
- [15] K. Shruti, S. Rajesh, G. R. Sabareesh, and P. N. Rao, "Study of Interference Effects on Chimneys," *J Phys Conf Ser*, vol. 1276, no. 1, p. 012033, Aug. 2019, <https://doi.org/10.1088/1742-6596/1276/1/012033>.
- [16] J. Franke, C. Hirsch, and M. Schatzmann, "Recommendations on the use of CFD in wind engineering," 2004. [Online]. Available: <https://www.researchgate.net/publication/251814717>
- [17] A. C. Khanduri, T. Stathopoulos, and C. B~dard, "interference effects a review of the Wind-induced on buildings-state-of-the-art," 1998.